

OPTICAL TOMOGRAPHIC RECONSTRUCTION USING THE P_N RADIATIVE TRANSFER EQUATION

S. WRIGHT, M. SCHWEIGER and S. ARRIDGE

Department of ,Computer Science, University College London, Gower Street, London, WC1E 6BT UK
e-mail: {S.Wright,M.Schweiger,S.Arridge}@cs.ucl.ac.uk

Abstract - In this paper we consider the inverse problem of reconstructing the absorption and scattering coefficients of the Radiative Transfer Equation (RTE) from measurements of photon current transmitted over a large number of scattering lengths. We consider an output least squares formulation of this problem and derive the appropriate forward operators and their Fréchet derivatives. For efficient implementation we derive the second order form of the RTE, and discuss its solution using a Finite Element Method (FEM). The P_N approximation is used to expand the radiance in spherical harmonics, which leads to a large sparse matrix system that can be efficiently solved. Examples are shown for a low-scattering case where the Diffusion Approximation fails.

1. INTRODUCTION

The concept of using optical radiation to penetrate highly scattering media, combined with image reconstruction methods to recover optical parameters inside the media, has been a recurrent idea for over a century. However it has received great attention in the last decade due to advances both in measurement technology and in theoretical and practical understanding of the nature of the image reconstruction problem. This field has come to be known as *Diffuse Optical Tomography* (DOT); for recent reviews see [1-3].

The term "Diffuse" is employed since the usual conditions being investigated are where the medium is so highly scattering that its propagation is nearly completely described by a Diffusion Approximation (DA). However, it is well known that under certain conditions, the DA is no longer valid. In particular the presence of non-scattering (void) regions, such as those occurring in the Cerebro-Spinal Fluid (CSF) filled ventricles in the brain, represent a situation for which the DA is clearly inadequate. Under these circumstances, more advanced methods are required [4-7].

A general model of light transport in scattering media, but one that ignores polarisation and coherence effects, is the Boltzmann Equation. This equation has been extensively studied in the field of Neutron Transport [8-12] and in Radiation transfer [13,14] where it is known as the Radiative Transfer Equation (RTE). Although a very large literature exists on numerical methods for this problem, relatively little has been applied to Optical Tomography. First order methods based on finite differences for the steady state problem were studied in [6,15], and for the time dependent problem in [5]. In the frequency domain a first order finite volume method was developed in [16], and a finite element method in [17]. A finite element method for second order form based on the P_N approximations was developed in [18], and its application to Optical Tomography in the steady state and in the time domain was pioneered in [19-23]. The same method, taken to the P_3 approximation was studied in [24]. A second order form, using finite elements, but using discrete ordinates for the angular variable was studied in [25]. In this paper, we use the second order P_N formulation in the frequency domain, and discuss its application to the inverse problem.

2. FORMULATION OF THE PROBLEM

We are considering the RTE in a domain Ω with boundary $\partial\Omega$, with outward normal $\hat{\nu}$. We will discuss only the *single-group* RTE which in the steady state is written

$$\left(\hat{\mathbf{s}} \cdot \nabla + \mu_{\text{tr}}(\mathbf{r}) + \frac{i\omega}{c} \right) \phi(\mathbf{r}, \hat{\mathbf{s}}; \omega) = \mu_{\text{s}}(\mathbf{r}) \int_{S^2} \Theta(\hat{\mathbf{s}}, \hat{\mathbf{s}}') \phi(\mathbf{r}, \hat{\mathbf{s}}'; \omega) d\hat{\mathbf{s}}' + q(\mathbf{r}, \hat{\mathbf{s}}; \omega) \quad (1)$$

Here $\mu_{\text{tr}}(\mathbf{r}) = \mu_{\text{s}}(\mathbf{r}) + \mu_{\text{a}}(\mathbf{r})$ (units of inverse length) is the attenuation coefficient at position \mathbf{r} , with $\mu_{\text{s}}(\mathbf{r})$ the scattering coefficient and $\mu_{\text{a}}(\mathbf{r})$ the absorption coefficient. $\phi(\mathbf{r}, \hat{\mathbf{s}}; \omega)$ (units of inverse length cubed per steradian) is the number of photons per unit volume at position \mathbf{r} with velocity in angular direction $\hat{\mathbf{s}}$, with $q(\mathbf{r}, \hat{\mathbf{s}}; \omega)$ the number of source photons, and ω the modulation frequency. $\Theta(\hat{\mathbf{s}}, \hat{\mathbf{s}}')$ is the normalised phase function representing the probability of scattering from direction $\hat{\mathbf{s}}'$ to direction $\hat{\mathbf{s}}$.

In general, the phase function depends on the absolute angle $\hat{\mathbf{s}}$ and leads to anisotropic effects [26], but in this paper we will make the usual assumption of directional independent scattering $\Theta(\hat{\mathbf{s}}, \hat{\mathbf{s}}') \equiv \Theta(\hat{\mathbf{s}} \cdot \hat{\mathbf{s}}') = \Theta(\cos \tau)$, whereupon the integral operator can be interpreted as a convolution on S^2 and is defined by

$$\mathcal{S}[\phi](\hat{\mathbf{s}}) := \int_{S^2} \Theta(\hat{\mathbf{s}} \cdot \hat{\mathbf{s}}') \phi(\hat{\mathbf{s}}') d\hat{\mathbf{s}}' =: \Theta \odot \phi. \quad (2)$$

We define the combined attenuation and inscatter operator

$$\mathcal{C} := \tilde{\mu}_{\text{tr}}(\omega) - \mu_s \mathcal{S} = \mu_a + \frac{i\omega}{c} + \mu_s (\mathcal{I} - \mathcal{S}) \quad (3)$$

where $\tilde{\mu}_{\text{tr}}(\omega) := \mu_{\text{tr}} + \frac{i\omega}{c}$ is the complex attenuation coefficient. This allows us to write (1) as

$$\hat{\mathbf{s}} \cdot \nabla \phi(\mathbf{r}, \hat{\mathbf{s}}; \omega) + \mathcal{C} \phi(\mathbf{r}, \hat{\mathbf{s}}; \omega) = q(\mathbf{r}, \hat{\mathbf{s}}; \omega). \quad (4)$$

The simplest boundary condition for the RTE is the *vacuum boundary condition* that specifies that there is no incoming energy flux crossing the boundary

$$\phi(\mathbf{r}, \hat{\mathbf{s}}; \omega) = 0 \quad \mathbf{r} \in \partial\Omega, \quad \forall \hat{\mathbf{s}} \cdot \hat{\nu} < 0. \quad (5)$$

We define the inward and outward fluxes :

$$J_+ = \int_{\hat{\mathbf{s}} \cdot \hat{\nu} > 0} (\hat{\mathbf{s}} \cdot \hat{\nu}) \phi(\mathbf{r}, \hat{\mathbf{s}}; \omega), \quad J_- = \int_{\hat{\mathbf{s}} \cdot \hat{\nu} < 0} (\hat{\mathbf{s}} \cdot -\hat{\nu}) \phi(\mathbf{r}, \hat{\mathbf{s}}; \omega), \quad J_n = J_+ - J_- . \quad (6)$$

The *Forward Operator* F_j is a non-linear mapping from pairs of functions in the solution space, to data on the boundary, for given incoming radiation η_j .

The *Direct Fréchet Derivative* $F'_j(\mu_a, \mu_s; \omega)$ is a linear mapping from pairs of functions in the solution space, to data on the boundary, for given incoming radiation η_j . F'_j is the linearisation of F_j around the solution point $\{\mu_a, \mu_s\}$ that maps changes in solution space functions to changes in data. The value of the mapping

$$y_j^\delta(\mathbf{m}; \omega) = F'_j(\mu_a, \mu_s; \omega) \begin{pmatrix} \alpha \\ \gamma \end{pmatrix}$$

is given by

$$\begin{aligned} & \left(\frac{i\omega}{c} + \hat{\mathbf{s}} \cdot \nabla + \mu_a(\mathbf{r}) + \mu_s(\mathbf{r}) \right) \phi_j^\delta(\mathbf{r}, \hat{\mathbf{s}}; \omega) - \mu_s(\mathbf{r}) \int_{S^2} \Theta(\hat{\mathbf{s}} \cdot \hat{\mathbf{s}}') \phi_j^\delta(\mathbf{r}, \hat{\mathbf{s}}', \omega) d\hat{\mathbf{s}}' = \\ & - \left(\frac{i\omega}{c} + \hat{\mathbf{s}} \cdot \nabla + \alpha(\mathbf{r}) + \gamma(\mathbf{r}) \right) \phi_j(\mathbf{r}, \hat{\mathbf{s}}; \omega) + \gamma(\mathbf{r}) \int_{S^2} \Theta(\hat{\mathbf{s}} \cdot \hat{\mathbf{s}}') \phi_j(\mathbf{r}, \hat{\mathbf{s}}', \omega) d\hat{\mathbf{s}}' \quad \mathbf{r} \in \Omega \setminus \partial\Omega \quad (7) \end{aligned}$$

$$\phi_j^\delta(\mathbf{r}, \hat{\mathbf{s}}, \omega) = 0 \quad \text{on } \partial\Omega \times \{\hat{\mathbf{s}} \cdot \hat{\nu} < 0\} \quad (8)$$

$$y_j^\delta(\mathbf{m}; \omega) = \int_{\hat{\mathbf{s}} \cdot \hat{\nu} > 0} (\hat{\mathbf{s}} \cdot \hat{\nu}) \phi_j^\delta(\mathbf{m}, \hat{\mathbf{s}}; \omega), \quad \mathbf{m} \in \partial\Omega. \quad (9)$$

The *Adjoint Fréchet Derivative* $F_j'^*(\mu_a, \mu_s; \omega)$ is a linear mapping from functions on the boundary to pairs of functions in the solution space, for given incoming radiation η_j .

The value of the mapping

$$\begin{pmatrix} \alpha \\ \gamma \end{pmatrix} = F_j'^*(\mu_a, \mu_s; \omega) y_j^\delta(\mathbf{m}; \omega)$$

is given by

$$\left(-\frac{i\omega}{c} - \hat{\mathbf{s}} \cdot \nabla + \mu_a(\mathbf{r}) + \mu_s(\mathbf{r}) \right) \psi_j(\mathbf{r}, \hat{\mathbf{s}}; \omega) - \mu_s(\mathbf{r}) \int_{S^2} \Theta(\hat{\mathbf{s}} \cdot \hat{\mathbf{s}}') \psi_j(\mathbf{r}, \hat{\mathbf{s}}', \omega) d\hat{\mathbf{s}}' = 0 \quad \mathbf{r} \in \Omega \setminus \partial\Omega \quad (10)$$

$$\psi_j(\mathbf{r}, \hat{\mathbf{s}}, \omega) = \overline{y_j^\delta(\mathbf{m}; \omega)} \quad \text{on } \partial\Omega \times \{\hat{\mathbf{s}} \cdot \hat{\nu} > 0\} \quad (11)$$

$$\begin{pmatrix} \alpha \\ \gamma \end{pmatrix} = \int_{S^2} \begin{pmatrix} -\overline{\psi_j} \phi_j \\ \overline{\psi_j} (\int_{S^2} \Theta(\hat{\mathbf{s}} \cdot \hat{\mathbf{s}}') \phi_j d\hat{\mathbf{s}}' - \phi_j) \end{pmatrix} d\hat{\mathbf{s}} \quad \mathbf{r} \in \Omega \setminus \partial\Omega. \quad (12)$$

3. THE INVERSE PROBLEM

We consider the regularised output least-squares approach to the inverse problem. We assume a finite number of incoming radiation sources $\{\eta_j; j = 1 \dots S\}$. The forward operator is now considered as a stacked set of operators

$$\mathbf{y}(\mathbf{m}; \omega) = \begin{bmatrix} y_1(\mathbf{m}; \omega) \\ y_2(\mathbf{m}; \omega) \\ \vdots \\ y_S(\mathbf{m}; \omega) \end{bmatrix} = \mathbf{F}(\mu_a, \mu_s; \omega) = \begin{bmatrix} F_1(\mu_a, \mu_s; \omega) \\ F_2(\mu_a, \mu_s; \omega) \\ \vdots \\ F_S(\mu_a, \mu_s; \omega) \end{bmatrix}. \quad (13)$$

We also consider a finite sampling of the outgoing distributions $y_j(\mathbf{m}; \omega)$, leading to a *measurement model*

$$y_{j,i}(\omega) = \mathcal{M}_i [y_j(\mathbf{m}; \omega)] \int_{\partial\Omega} w_i(\mathbf{m}) y_j(\mathbf{m}; \omega) \quad (14)$$

where $w_i(\mathbf{m})$ represents the finite aperture of a detector. In the following we assume a finite number M of detectors, defined as a set of functions

$$\mathbb{W} = \{w(\mathbf{m})_k; k = 1 \dots M\},$$

with $\mathbb{W}_j \subset \mathbb{W}$ the subset of size M_j of detectors that see source j . We seek the solution

$$\{\hat{\mu}_a, \hat{\mu}_s\} = \underset{\{\mu_a, \mu_s\}}{\operatorname{argmin}} \sum_{i,j} |y_{j,i}(\omega) - F_{j,i}(\mu_a, \mu_s; \omega)|^2 + \lambda \mathcal{J}(\mu_a, \mu_s) \quad (15)$$

where $\mathcal{J}(\mu_a, \mu_s)$ is a regularising functional and $\lambda > 0$ is a regularisation parameter.

The Newton scheme for solving (15) reads

$$\begin{pmatrix} \mu_a \\ \mu_s \end{pmatrix}^{(k+1)} = \begin{pmatrix} \mu_a \\ \mu_s \end{pmatrix}^{(k)} + \tau \left(\mathbf{F}'^* \mathbf{F}' + \lambda \mathcal{J}'' \right)^{-1} \left[\mathbf{F}'^* (\mathbf{y} - \mathbf{F}) - \lambda \mathcal{J}' \right]. \quad (16)$$

A conventional way to implement this scheme is to build the explicit discrete representation of \mathbf{F}' referred to as the Jacobian \mathbf{J} . In this paper we use an adjoint method to construct the Jacobian (see section 5.4) and use a generalised minimum residual (GMRES) iterative linear solver to implement (16). The GMRES solver can be implemented in terms of matrix-vector and matrix-transpose-vector operations without explicitly constructing the Hessian term. We use an inexact line-search to determine τ at each iteration. The regularisation term \mathcal{J} was implemented as a second order Tikhonov scheme of the form

$$\mathcal{J}(\mu_a, \mu_s) = \langle \mathbf{L} \begin{pmatrix} \mu_a \\ \mu_s \end{pmatrix}, \begin{pmatrix} \mu_a \\ \mu_s \end{pmatrix} \rangle \quad (17)$$

with derivatives

$$\mathcal{J}'(\mu_a, \mu_s) = \mathbf{L} \begin{pmatrix} \mu_a \\ \mu_s \end{pmatrix}, \quad \mathcal{J}'' = \mathbf{L} \quad (18)$$

where \mathbf{L} is the discretised form of the Laplacian operator. The regularisation parameter λ can be evaluated for example by an L-curve method.

4. EVEN PARITY TRANSPORT EQUATION AND THE WEAK FORMULATION

For the use of numerical methods based on variational principles, it is convenient to work with a second-order, self-adjoint operator. To derive the even-parity RTE, we define even parity radiance and source terms

$$\phi^\pm(\hat{\mathbf{s}}) := \frac{1}{2} (\phi(\hat{\mathbf{s}}) \pm \phi(-\hat{\mathbf{s}})), \quad q^\pm(\hat{\mathbf{s}}) := \frac{1}{2} (q(\hat{\mathbf{s}}) \pm q(-\hat{\mathbf{s}})).$$

We may also split the kernel of the convolution operator as

$$\Theta^\pm(\cos \tau) = \frac{1}{2} (\Theta(\cos \tau) \pm \Theta(-\cos \tau)).$$

Then (2) becomes

$$\mathcal{S}[\phi] = \mathcal{S}^+[\phi^+] + \mathcal{S}^-[\phi^-] \quad (19)$$

where we have defined

$$\mathcal{S}^\pm[\phi^\pm](\hat{\mathbf{s}}) := \int_{S^2} \Theta^\pm(\hat{\mathbf{s}} \cdot \hat{\mathbf{s}}') \phi^\pm(\hat{\mathbf{s}}') d\hat{\mathbf{s}}' = \Theta^\pm \odot \phi^\pm. \quad (20)$$

Finally we can define

$$\mathcal{C}^\pm := \tilde{\mu}_{\text{tr}}(\omega) - \mu_s \mathcal{S}^\pm = \mu_a + \frac{i\omega}{c} + \mu_s (\mathcal{I} - \mathcal{S}^\pm). \quad (21)$$

The derivation of the even parity transport equation proceeds by defining the odd parity radiance in terms of the even parity radiance as

$$\phi^-(\hat{\mathbf{s}}) = \mathcal{D} [q^-(\hat{\mathbf{s}}) - \hat{\mathbf{s}} \cdot \nabla \phi^+(\hat{\mathbf{s}})] \quad (22)$$

where the generalised diffusion operator is defined $\mathcal{D} := (\mathcal{C}^-)^{-1}$. After elimination of terms we arrive at

$$(\mathcal{C}^+ - \hat{\mathbf{s}} \cdot \nabla (\mathcal{D} \hat{\mathbf{s}} \cdot \nabla)) \phi^+(\mathbf{r}, \hat{\mathbf{s}}; \omega) = q^+(\mathbf{r}, \hat{\mathbf{s}}; \omega) - \hat{\mathbf{s}} \cdot \nabla (\mathcal{D} q^-(\mathbf{r}, \hat{\mathbf{s}}; \omega)). \quad (23)$$

4.1 The Weak Formulation

In the weak formulation of the even parity RTE, the (even-parity) radiance is represented in a finite-dimensional space χ^{h+}

$$\phi^+(\mathbf{r}, \hat{\mathbf{s}}) \simeq \phi^{h+}(\mathbf{r}, \hat{\mathbf{s}}) = \sum_{k=1}^K \phi_k^+ f_k(\mathbf{r}, \hat{\mathbf{s}}) \quad (24)$$

where $\{f_k; k = 1, \dots, K\}$ are a set of basis functions for χ^{h+} . Let us assume that the basis is developed separately for the spatial and angular terms

$$f_k(\mathbf{r}, \hat{\mathbf{s}}) = u_d(\mathbf{r}) \theta_t(\hat{\mathbf{s}}) \quad d = 1, \dots, D; t = 1, \dots, T; K = D \times T. \quad (25)$$

Since we require even parity for ϕ^{h+} it is natural to choose θ_t to have even parity. The space χ^{h+} is equipped with a norm

$$\langle \psi, \phi \rangle := \int_{S^2} \int_{\Omega} \psi(\mathbf{r}, \hat{\mathbf{s}}) \phi(\mathbf{r}, \hat{\mathbf{s}}) d\mathbf{r} d\hat{\mathbf{s}}. \quad (26)$$

Since ϕ^{h+} is an approximation to ϕ^+ it does not satisfy (23) exactly, but rather

$$(\mathcal{C}^+ - \hat{\mathbf{s}} \cdot \nabla (\mathcal{D} \hat{\mathbf{s}} \cdot \nabla)) \phi^{h+}(\mathbf{r}, \hat{\mathbf{s}}; \omega) - q^{h+}(\mathbf{r}, \hat{\mathbf{s}}; \omega) + \eta^{h+}(\mathbf{r}, \hat{\mathbf{s}}; \omega) = e(\mathbf{r}, \hat{\mathbf{s}}; \omega) \quad (27)$$

where q^{h+} and η^{h+} are the projection onto χ^{h+} of q^+ and $\hat{\mathbf{s}} \cdot \nabla (\mathcal{D} q^-(\mathbf{r}, \hat{\mathbf{s}}; \omega))$, respectively.

The principle of the weak (Galerkin) approximation is that the error term $e(\mathbf{r}, \hat{\mathbf{s}}; \omega)$ be orthogonal to the space χ^{h+} , i.e. that

$$\langle f_k, e \rangle = 0 \quad \forall k = 1, \dots, K \quad (28)$$

which leads to a discrete matrix equation for the K unknowns ϕ_k^+

$$\mathbf{M} \phi^+ = \mathbf{q}^+. \quad (29)$$

Consider the weak version of the boundary conditions (5) :

$$\int_{\hat{\mathbf{s}} \cdot \hat{\nu} < 0} (\hat{\mathbf{s}} \cdot \hat{\nu}) \theta_t(\hat{\mathbf{s}}) \phi(\mathbf{r}, \hat{\mathbf{s}}; \omega) d\hat{\mathbf{s}} = 0 \quad t = 1, \dots, T. \quad (30)$$

Let us assume that $q = 0|_{\partial\Omega}$ then we have

$$\phi = \phi^+ + \phi^- = \phi^+ - \mathcal{D} \hat{\mathbf{s}} \cdot \nabla \phi^+,$$

so that (30) becomes

$$\begin{aligned} \int_{\hat{\mathbf{s}} \cdot \hat{\nu} < 0} (\hat{\mathbf{s}} \cdot \hat{\nu}) \theta_t(\hat{\mathbf{s}}) \phi^+(\mathbf{r}, \hat{\mathbf{s}}; \omega) d\hat{\mathbf{s}} &= \frac{1}{2} \int_{S^2} |\hat{\mathbf{s}} \cdot \hat{\nu}| \theta_t(\hat{\mathbf{s}}) \phi^+(\mathbf{r}, \hat{\mathbf{s}}; \omega) d\hat{\mathbf{s}} \\ \int_{\hat{\mathbf{s}} \cdot \hat{\nu} < 0} (\hat{\mathbf{s}} \cdot \hat{\nu}) \theta_t(\hat{\mathbf{s}}) \mathcal{D}\hat{\mathbf{s}} \cdot \nabla \phi^+(\mathbf{r}, \hat{\mathbf{s}}; \omega) d\hat{\mathbf{s}} &= \frac{1}{2} \int_{S^2} (\hat{\mathbf{s}} \cdot \hat{\nu}) \theta_t(\hat{\mathbf{s}}) \mathcal{D}\hat{\mathbf{s}} \cdot \nabla \phi^+(\mathbf{r}, \hat{\mathbf{s}}; \omega) d\hat{\mathbf{s}} \quad t = 1, \dots, T. \end{aligned} \quad (31)$$

From the Galerkin formulation, we can write (28) as

$$\langle u_d \theta_t, (\mathcal{C}^+ - \hat{\mathbf{s}} \cdot \nabla \mathcal{D}\hat{\mathbf{s}} \cdot \nabla) \phi^{h+} \rangle = \langle u_d \theta_t, q^+ \rangle. \quad (32)$$

Applying the Divergence Theorem ($\int_{\Omega} \hat{\mathbf{s}} \cdot \nabla g = \int_{\partial\Omega} \hat{\mathbf{s}} \cdot \hat{\nu} g$) and making use of (31) we get

$$\langle u_d \theta_t, \mathcal{C}^+ \phi^{h+} \rangle + \langle \hat{\mathbf{s}} \cdot \nabla u_d \theta_t, \mathcal{D}\hat{\mathbf{s}} \cdot \nabla \phi^{h+} \rangle + \int_{S^2} |\hat{\mathbf{s}} \cdot \hat{\nu}| \theta_t(\hat{\mathbf{s}}) \int_{\partial\Omega} u_d(\mathbf{r}) \phi^+(\mathbf{r}, \hat{\mathbf{s}}; \omega) d\mathbf{r} d\hat{\mathbf{s}} = \langle u_d \theta_t, q^+ \rangle. \quad (33)$$

4.2 Measurement Operator

For the even-parity form of the Boltzmann Equation we have

$$\phi(\mathbf{r}, \hat{\mathbf{s}}; \omega) \simeq \phi^+(\mathbf{r}, \hat{\mathbf{s}}; \omega) - \mathcal{D}(\mathbf{r}) \hat{\mathbf{s}} \cdot \nabla \phi^+(\mathbf{r}, \hat{\mathbf{s}}; \omega) \quad (34)$$

whence

$$\begin{aligned} J_+ = J_n(\mathbf{r}; \omega) &= -\mathcal{D}(\mathbf{r}) \int_{S^2} (\hat{\mathbf{s}} \cdot \hat{\nu}) \hat{\mathbf{s}} \cdot \nabla \phi^+(\mathbf{r}, \hat{\mathbf{s}}; \omega) d\hat{\mathbf{s}} = -2 \int_{\hat{\mathbf{s}} \cdot \hat{\nu} < 0} (\hat{\mathbf{s}} \cdot \hat{\nu}) \phi^+(\mathbf{r}, \hat{\mathbf{s}}; \omega) d\hat{\mathbf{s}} \\ &= - \int_{S^2} |\hat{\mathbf{s}} \cdot \hat{\nu}| \phi^+(\mathbf{r}, \hat{\mathbf{s}}; \omega) d\hat{\mathbf{s}}. \end{aligned} \quad (35)$$

5. IMPLEMENTATION

5.1 P_N Approximation

In principle we may use any basis functions $\theta_t(\hat{\mathbf{s}})$ for the angular variable. However if we use spherical harmonics we obtain the so-called P_N approximations. We express the quantities in (1) as

$$\phi(\mathbf{r}, \hat{\mathbf{s}}; \omega) = \sum_l \sum_{m=-l}^l \left(\frac{2l+1}{4\pi} \right)^{\frac{1}{2}} \phi_{l,m}(\mathbf{r}; \omega) Y_{l,m}(\hat{\mathbf{s}}) \quad (36)$$

$$q(\mathbf{r}, \hat{\mathbf{s}}; \omega) = \sum_l \sum_{m=-l}^l \left(\frac{2l+1}{4\pi} \right)^{\frac{1}{2}} q_{l,m}(\mathbf{r}; \omega) Y_{l,m}(\hat{\mathbf{s}}) \quad (37)$$

where $Y_{l,m}(\hat{\mathbf{s}})$ is a spherical harmonic of order l degree m , and the normalisation factor $((2l+1)/4\pi)^{1/2}$ is introduced for convenience. If the phase function is assumed to be independent of the explicit angle $\hat{\mathbf{s}}$ and is written $\Theta(\hat{\mathbf{s}} \cdot \hat{\mathbf{s}}')$ then

$$\Theta(\hat{\mathbf{s}} \cdot \hat{\mathbf{s}}') = \sum_l \sum_{m=-l}^l \Theta_l \bar{Y}_{l,m}(\hat{\mathbf{s}}') Y_{l,m}(\hat{\mathbf{s}})$$

and (1) can be expressed as an infinite set of coupled first order equations. When these are truncated by assuming $\phi_{l,m} = 0; l > N$ for some N the result is a set of $(N+1)^2$ (in 3D) first order equations known as the P_N approximation [2, 8, 10].

The \mathcal{P}_N operator has a special form

$$\mathcal{P}_N = \begin{bmatrix} \mathcal{C}_0 & \mathcal{A}_0 & 0 & 0 & \dots \\ \mathcal{A}_0^T & 3\mathcal{C}_1 & 3\mathcal{A}_1 & 0 & \dots \\ 0 & 3\mathcal{A}_1^T & 5\mathcal{C}_2 & 5\mathcal{A}_2 & \dots \\ \vdots & \vdots & \vdots & \vdots & \vdots \end{bmatrix}. \quad (38)$$

The operator \mathcal{C}_l is diagonal for angularly independent scattering and is given by

$$\mathcal{C}_l = \left(\mu_a + (1 - \Theta_l) \mu_s + \frac{i\omega}{c} \right) \mathcal{I}_l$$

where \mathcal{I}_1 is the $(2l+1) \times (2l+1)$ identity operator. The operator \mathcal{A}_1 is a generalisation of the divergence operator and has the following form

$$\mathcal{A}_1 = \begin{bmatrix} \alpha_{l,-l} \mathcal{D}_\xi^+ & \beta_{l,-l} \frac{\partial}{\partial z} & \gamma_{l,-l} \mathcal{D}_\xi^- & 0 & \dots \\ 0 & \alpha_{l,1-l} \mathcal{D}_\xi^+ & \beta_{l,1-l} \frac{\partial}{\partial z} & \gamma_{l,1-l} \mathcal{D}_\xi^- & \dots \\ \vdots & \vdots & \vdots & \vdots & \vdots \\ \dots & 0 & \alpha_{l,l} \mathcal{D}_\xi^+ & \beta_{l,l} \frac{\partial}{\partial z} & \gamma_{l,l} \mathcal{D}_\xi^- \end{bmatrix} \quad (39)$$

where

$$\alpha_{l,m} = \frac{\sqrt{(l-m+2)(l-m+1)}}{2l+1}, \quad \beta_{l,m} = \frac{\sqrt{(l+1-m)(l+1+m)}}{2l+1}, \quad \gamma_{l,m} = \frac{\sqrt{(l+m+1)(l+m+2)}}{2l+1},$$

$$\mathcal{D}_\xi^+ = \frac{-1}{2} \left(\frac{\partial}{\partial x} + i \frac{\partial}{\partial y} \right), \quad \mathcal{D}_\xi^- = \frac{-1}{2} \left(\frac{\partial}{\partial x} - i \frac{\partial}{\partial y} \right) 1.$$

Applying the representation (38) to the even-parity form of the RTE leads to the system

$$\begin{bmatrix} \mathcal{P}_{0,0}^+ & \mathcal{P}_{0,2}^+ & 0 & 0 & \dots \\ \mathcal{P}_{2,0}^+ & \mathcal{P}_{2,2}^+ & \mathcal{P}_{2,4}^+ & 0 & \dots \\ 0 & \mathcal{P}_{4,2}^+ & \mathcal{P}_{4,4}^+ & \mathcal{P}_{4,6}^+ & \dots \\ \vdots & \vdots & \vdots & \vdots & \vdots \end{bmatrix} \begin{bmatrix} \phi_{0,0}^+ \\ \phi_{2,m \in [-2,2]}^+ \\ \phi_{4,m \in [-4,4]}^+ \\ \vdots \end{bmatrix} = \begin{bmatrix} q_{0,0}^+ \\ q_{2,m \in [-2,2]}^+ \\ q_{4,m \in [-4,4]}^+ \\ \vdots \end{bmatrix} \quad (40)$$

where

$$\begin{aligned} \mathcal{P}_{0,0}^+ &= \mathcal{C}_0 - \frac{1}{3} \mathcal{A}_0 \mathcal{C}_1^{-1} \mathcal{A}_0^T & \mathcal{P}_{0,2}^+ &= -\mathcal{A}_0 \mathcal{C}_1^{-1} \mathcal{A}_1 \\ \mathcal{P}_{2,0}^+ &= -\mathcal{A}_1^T \mathcal{C}_1^{-1} \mathcal{A}_0^T & \mathcal{P}_{2,2}^+ &= 5\mathcal{C}_2 - 3\mathcal{A}_1^T \mathcal{C}_1^{-1} \mathcal{A}_1 - \frac{25}{7} \mathcal{A}_2 \mathcal{C}_3^{-1} \mathcal{A}_2^T \\ & \dots & & \dots \end{aligned}$$

5.2 Even to Odd Calculation

In the Even Parity formulation presented in this paper only the even components of the spherical harmonic expansion of the radiance $\phi(\mathbf{r}, \hat{\mathbf{s}}; \omega)$ are calculated. However, in order to evaluate the Fréchet Derivatives, (12) the odd components of the spherical harmonic expansion of $\phi(\mathbf{r}, \hat{\mathbf{s}}; \omega)$ are needed. In order to evaluate the odd components, expression (22) is used to compute the odd components directly from the even components. The transport term ($\hat{\mathbf{s}} \cdot \nabla$) is evaluated using the usual spherical harmonic angular basis and is given by (39). Hence there is a requirement to evaluate x,y and z derivatives of the Even Parity components. This is accomplished by implementing a central difference scheme or a relevant forward/backward scheme at the boundaries.

5.3 Finite Element Method (FEM)

The FEM implementation of (40) is obtained by specifying that the domain Ω is divided into P elements, joined at D vertex nodes and the basis functions $\{u_d(\mathbf{r}); d = 1 \dots D\}$ are chosen to have limited support. The problem of solving for ϕ^{b+} becomes one of sparse matrix inversion for which standard methods are readily available. Because of the separability of the spatial and angular basis functions, the matrix \mathbf{M} in (29) has the structure of a $D \times D$ graph representing the connectivity of the FEM mesh. For the general P_N equations each node that is not on the boundary needs to be expanded into a $T \times T$ block whose structure has the block tridiagonal form shown in (40); this block is also sparse, with the proportion of non-zeroes decreasing with increasing P_N order.

Whereas the integration of products of spherical harmonic functions on the sphere is given analytically, the implementation of the boundary conditions calls for the integration on a half-sphere of the surface integral in (33). For this a Lebedev-Skorokhodo quadrature [27] is employed.

5.4 Calculation of the Jacobian

Each row of the Jacobian is a pair of functions $\begin{pmatrix} \rho_a(\mathbf{r}) \\ \rho_s(\mathbf{r}) \end{pmatrix}_{i,j}$ in space, which is obtained by constructing adjoint source vectors ϕ_i^* for each measurement position as follows

$$\left(-\frac{i\omega}{c} - \hat{\mathbf{s}} \cdot \nabla + \mu_a(\mathbf{r}) + \mu_s(\mathbf{r}) \right) \phi_i^*(\mathbf{r}, \hat{\mathbf{s}}; \omega) - \mu_s(\mathbf{r}) \int_{S^2} \Theta(\hat{\mathbf{s}} \cdot \hat{\mathbf{s}}') \phi_i^*(\mathbf{r}, \hat{\mathbf{s}}', \omega) d\hat{\mathbf{s}}' = 0 \quad \mathbf{r} \in \Omega \setminus \partial\Omega \quad (41)$$

$$\phi_i^*(\mathbf{r}, \hat{\mathbf{s}}, \omega) = w_i(\mathbf{m}) \quad \text{on } \partial\Omega \times \{\hat{\mathbf{s}} \cdot \hat{\nu} > 0\} \quad (42)$$

$$\begin{pmatrix} \rho_a(\mathbf{r}) \\ \rho_s(\mathbf{r}) \end{pmatrix}_{i,j} = \int_{S^2} \begin{pmatrix} -\phi_i^* \phi \\ \overline{\phi_i^*} (\int_{S^2} \Theta(\hat{\mathbf{s}} \cdot \hat{\mathbf{s}}') \phi d\hat{\mathbf{s}}' - \phi) \end{pmatrix} d\hat{\mathbf{s}} \quad \mathbf{r} \in \Omega \setminus \partial\Omega. \quad (43)$$

Using the spherical harmonic representation (36) we can represent (43) as

$$\begin{pmatrix} \rho_a(\mathbf{r}) \\ \rho_s(\mathbf{r}) \end{pmatrix}_{i,j} = \begin{pmatrix} -\sum_{l,m} \overline{\phi_{l,m}^*(\mathbf{r};\omega)} \phi_{l,m}(\mathbf{r};\omega) \\ \sum_{l,m} (1 - \Theta_l) \overline{\phi_{l,m}^*(\mathbf{r};\omega)} \phi_{l,m}(\mathbf{r};\omega) \end{pmatrix} \quad \mathbf{r} \in \Omega \setminus \partial\Omega. \quad (44)$$

Note that the odd components of the radiance are needed here.

In order to deal with the large dynamic range of the data we make use of the logarithm of the data which leads to rescaling of the Jacobian by the data. And in order to deal with the mapping from real coefficients to complex data we split the Jacobian into real and imaginary parts. This leads to the following linear system

$$\begin{pmatrix} \text{Re} [\log \mathbf{y}^\delta] \\ \text{Im} [\log \mathbf{y}^\delta] \end{pmatrix} = \begin{pmatrix} \text{Re} \left[\text{diag} \left\{ \frac{1}{\mathbf{y}} \right\} \mathbf{J} \right] \\ \text{Im} \left[\text{diag} \left\{ \frac{1}{\mathbf{y}} \right\} \mathbf{J} \right] \end{pmatrix} \begin{pmatrix} \alpha \\ \gamma \end{pmatrix}. \quad (45)$$

6. RESULTS

The above theory has been applied to a simple test problem to produce some initial results. A cube of side length 10mm and background optical parameters $\mu_a = 0.025\text{mm}^{-1}$ and $\mu_s = 0.75\text{mm}^{-1}$ was considered. Two spherical objects of radius 3mm were inserted at diagonally opposite locations. Object 1, centred at (-2,-2,-2) had increased absorption coefficient : $\mu_a = 0.075\text{mm}^{-1}$ and $\mu_s = 0.75\text{mm}^{-1}$, and object 2 centred at (2,2,2) had decreased scattering coefficient : $\mu_a = 0.025\text{mm}^{-1}$ and $\mu_s = 0.25\text{mm}^{-1}$. Figure 1 shows an illustration of the domain described. Four sources were placed on the edges of a square with four detectors on the vertices of the square on each of the four vertical sides of the domain, making a total of 16 sources and 16 detectors in total. The refractive index of the medium was taken to be 1.0

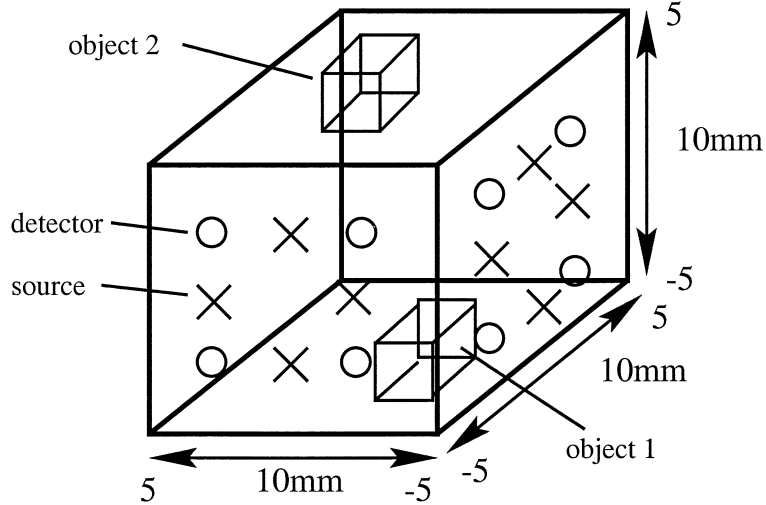


Figure 1: The solution domain.

with the sources taken to have a frequency of 100MHz. The angular distribution of the source structure was taken to be isotropic for all forward models in both data generation and reconstruction. Data was simulated at the 16 detectors for each source using the P_5 model, leading to 256 measurements for both log amplitude and phase, and is shown in Figure 2. 1% Gaussian multiplicative noise was added to the data, and reconstruction was performed for both μ_a , and μ_s simultaneously, starting from the background state of $\mu_a = 0.025\text{mm}^{-1}$ and $\mu_s = 0.75\text{mm}^{-1}$. Two reconstructions were calculated, firstly using the P_1 reconstruction model and secondly using the P_3 reconstruction model. Figure 3 and Figure 4 show the reconstructions for the absorption and scattering parameters respectively, for the two different models. In both cases the result is for the fourth iteration of the Newton scheme. The results presented consist of a cross-section of the domain through the plane $z = -2$ for μ_a and $z = 2$ for μ_s . Both reconstructions seem to produce reasonable results and are qualitatively similar in structure. A smoothing effect is clearly seen on the reconstructed object, i.e. the sharp edges of the inserted low scatter region are not determined. This is due to the ill-posedness of the system and the use of a Tikhonov regularisation scheme which suppresses the high frequencies in the solution. Artefacts were noticeably more prevalent in the P_1 reconstruction because of the lower accuracy of the model fit.

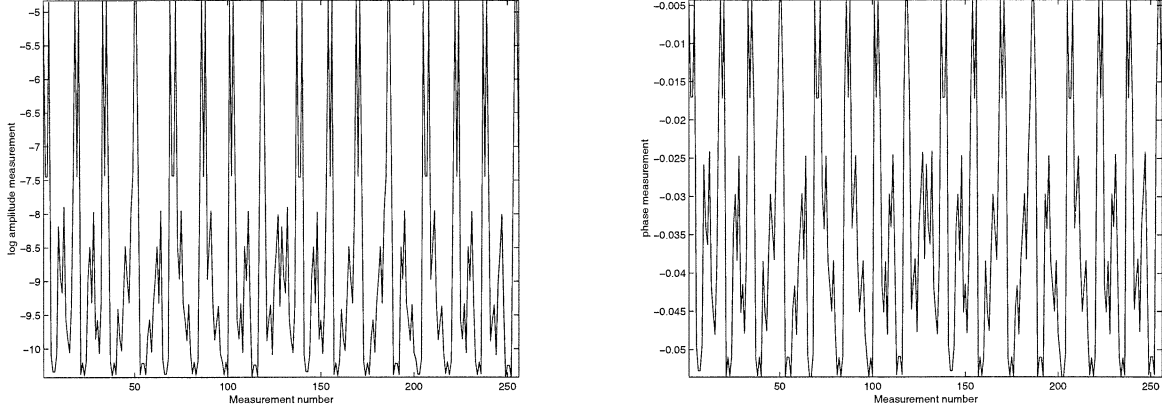


Figure 2: The log amplitude and phase data calculated using the P_3 forward model.

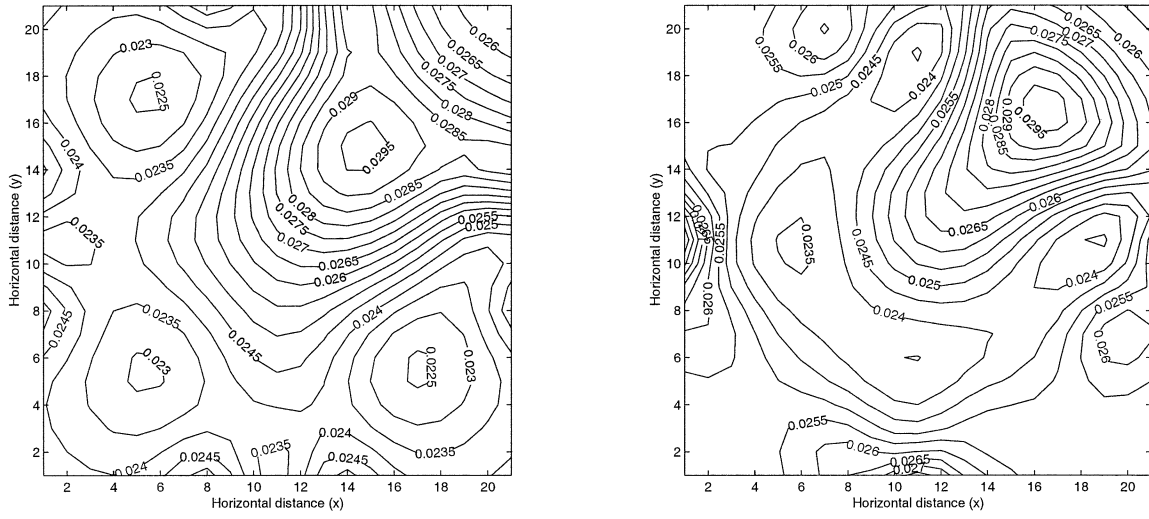


Figure 3: The absorption parameter, μ_a , calculated using the P_1 and P_3 reconstruction models.

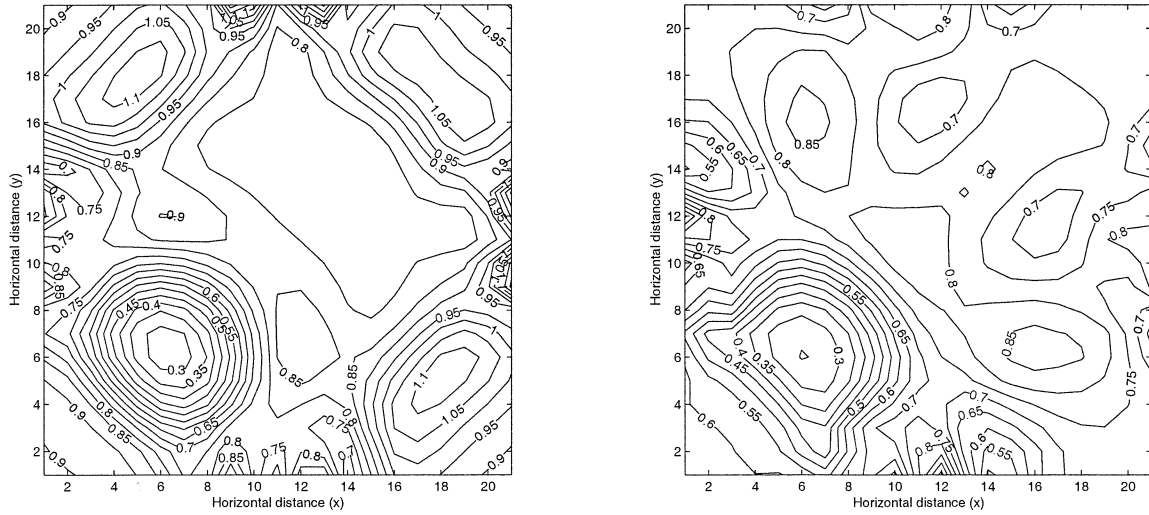


Figure 4: The scatter parameter, μ_s , calculated using the P_1 and P_3 reconstruction models.

To examine the differences more accurately Figure 5 shows the one dimensional cross-sections for μ_a and μ_s through the centres of the two objects. Figure 5 shows that both models underestimate the μ_a object but produce a good estimate to the low scattering region $\mu_s = 0.25mm^{-1}$ with the P_3 reconstruction

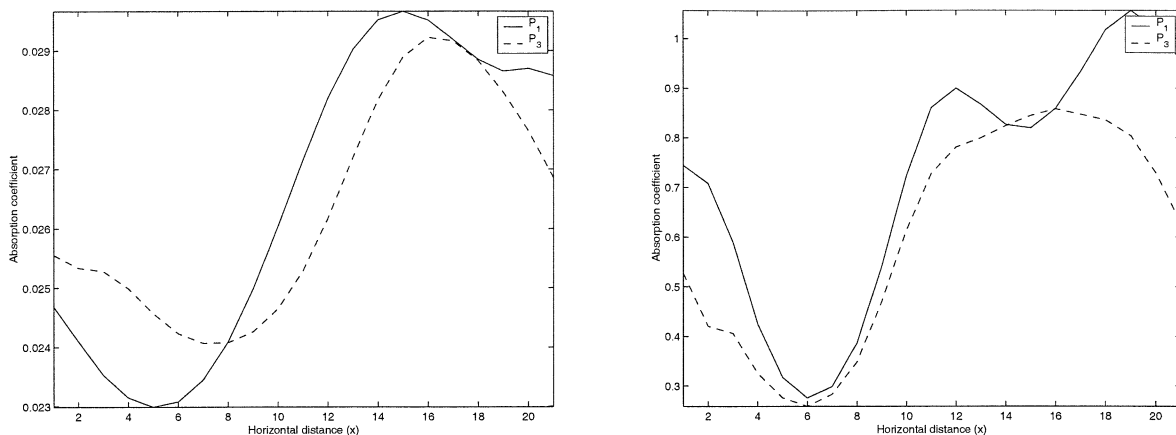


Figure 5: The cross-section of the absorption and scatter parameters, μ_a and μ_s , calculated using the P_1 and P_3 reconstruction models.

model producing a marginally lower value. Further investigations are needed to test whether the higher order reconstruction schemes can produce superior results for domains which have low scatter regions. Future work will test this method with simulated data obtained from another source, such as a Monte Carlo methods, and with measured data.

7. CONCLUSIONS

In this paper we presented the derivation of the forward and inverse models for the reconstruction of absorbing and scattering coefficients of the RTE. The implementation was in terms of a FEM for the second order even-parity RTE, using the P_N approximations. This leads to a large sparse matrix system with a simple structure. We have reported initial results that show the improvement of the RTE method over the simple DA.

Acknowledgement

The authors would like to acknowledge financial support received from EPSRC grants GR/R86201/01 and GR/N14248/01. We thank Oliver Dorn and Cassiano de Oliveira for many useful discussions on inverse transport problems and FEM implementations.

REFERENCES

1. S. R. Arridge and J. C. Hebden, Optical imaging in medicine: II. Modelling and reconstruction. *Phys. Med. Biol.* (1997) **42**, 841–853.
2. S. R. Arridge, Optical tomography in medical imaging. *Inverse Problems* (1999) **15**(2), R41–R93.
3. D. A. Boas, D. H. Brooks, E. L. Miller, C. A. DiMarzio, M. Kilmer, R. J. Gaudette and Q. Zhang, Imaging the body with diffuse optical tomography. *IEEE Sig. Proc. Magazine* (2001) **18**(6), 57–75.
4. M. Firbank, S. R. Arridge, M. Schweiger and D. T. Delpy, An investigation of light transport through scattering bodies with non-scattering regions. *Phys. Med. Biol.* (1996) **41**, 767–783.
5. O. Dorn, A transport-backtransport method for optical tomography. *Inverse Problems* (1998) **14**(5), 1107–1130.
6. A. H. Hielscher, R. E. Alcouffe and R. L. Barbour, Comparison of finite-difference transport and diffusion calculations for photon migration in homogeneous and heterogeneous tissue. *Phys. Med. Biol.* (1998) **43**, 1285–1302.
7. S. R. Arridge, H. Dehghani, M. Schweiger and E. Okada, The finite element model for the propagation of light in scattering media : A direct method for domains with non-scattering regions. *Med. Phys.* (2000) **27**(1), 252–264.
8. B. Davison, *Neutron Transport Theory*, Oxford University Press, London, 1957.

9. A. M. Weinberg and E. P. Wigner, *The Physical Theory of Neutron Chain Reactors*, University of Chicago Press, 1958.
10. M. C. Case and P. F. Zweifel, *Linear Transport Theory*, Addison-Wesley, New York, 1967.
11. J. J. Duderstadt and W. R. Martin, *Transport Theory*, John Wiley & Sons, New York, 1979.
12. R. T. Ackroyd, *Finite Element Methods for Particle Transport : Applications to Reactor and Radiation Physics*, Research Studies Press Ltd., Taunton, 1997.
13. S. Chandrasekhar, *Radiative Transfer*, Oxford University Press, London, 1950.
14. A. Ishimaru, *Wave Propagation and Scattering in Random Media*, Vol. 1, Academic, New York, 1978.
15. A. D. Klose, U. Netz, J. Beuthan and A. H. Hielscher, Optical tomography using the time-independent equation of radiative transfer - Part 1 : Forward model. *J. Quantitative Spectroscopy and Radiative Transfer* (2002) **72**, 691–713.
16. K. Ren, G. S. Abdoulaev, G. Bal and A. Hielscher, Algorithm for solving the equation of radiative transfer in the frequency domain. *Opt. Lett.* (2004) **29**(6), 578–580.
17. T. Tarvainen, M. Vauhkonen, V. Kolehmainen and J. P. Kaipio, A hybrid radiative transfer - diffusion model for optical tomography. *Appl. Opt.* (2005) **44**(6), 876–886.
18. C. R. E. de Oliveira, An arbitrary geometry finite element method for multigroup neutron transport with anisotropic scattering. *Prog. Nucl. Energy* (1986) **18**, 227–236.
19. K. B. Tahir, C. R. E. de Oliveira, S. Katsimichas and J. C. Dainty, A comparison between finite element transport and Monte Carlo solutions for photon propagation, In *Proceedings of Applied Optics and Optoelectronics*, 1996, pp. 58–63.
20. C. R. E. de Oliveira and K. B. Tahir, Higher-order transport approximations for optical tomography, In *Proceedings of BiOS Europe '97, San Remo*, SPIE Bellingham WA, 1997, Vol. **3194**, pp. 212–218.
21. E. D. Aydin, *A Higher-Order Transport Model for Photon Propagation and its Applications to Optical Tomography*, PhD thesis, University of London., 1999.
22. E. D. Aydin, C.R.E. de Oliveira and A. J. H. Goddard, A comparison between transport and diffusion calculations using a finite element-spherical harmonics radiation transport method. *Med. Phys.* (2002) **2**(9), 2013–2023.
23. E. D. Aydin, C.R.E. de Oliveira and A. J. H. Goddard, A finite element-spherical harmonic radiation transport model for photon migration in turbid media. *J. Quantitative Spectroscopy and Radiative Transfer* (2004) **84**, 247–260.
24. H. Jiang, Optical image reconstruction based on the third-order diffusion equations. *Opt. Express*, (1999), **4**(8), 241–246.
25. G. S. Abdoulaev and A. H. Hielscher, Three-dimensional optical tomography with the equation of radiative transfer. *J. Electronic Imaging*, (2003), **12**(4), 594–601.
26. J. Heino, S.R. Arridge, J. Sikora and E. Somersalo, Anisotropic effects in highly scattering media. *Physical Review E* (2003) **68**, Article number 31908.
27. V. I. Lebedev and A.L.Skorokhodov, Quadrature formulas of orders 41,47 and 53 for the sphere. *Russian Acad. Sci. Dokl. Math.* (2002) **45**(3), 587–592.